**Supporting Information for:**

# Fate of Liposomes in the Presence of Phospholipase C and D: From Atomic to Supramolecular Lipid Arrangement

Margaret N. Holme[1,2,3,4], M. Harunur Rashid[5], Michael R. Thomas[1,2,3], Hanna M. G. Barriga[4], Karla–Luise Herpoldt[1,2,3], Richard K. Heenan[6], Cécile A. Dreiss[7], José Leobardo Bañuelos[6,8], Hai-nan Xie[1,2,3], Irene Yarovsky[5]* & Molly M. Stevens[1,2,3,4]**

[1]Department of Materials, Imperial College London, London, SW7 2AZ, UK
[2]Department of Bioengineering and [3]Institute of Biomedical Engineering, Imperial College London, London, SW7 2AZ, UK
[4]Department of Medical Biochemistry and Biophysics, Karolinska Institutet, SE-171 77 Stockholm, Sweden
[5]School of Engineering, RMIT University, Melbourne, Victoria, 3001, Australia
[6]STFC ISIS Facility, Rutherford Appleton Laboratory, Chilton, Didcot, OX11 0QX, UK
[7]School of Cancer and Pharmaceutical Sciences, King's College London, London SE1 9NH, UK
[8]Department of Physics, The University of Texas at El Paso, El Paso, Texas 79968, USA

Correspondence to:

* Email: irene.yarovsky@rmit.edu.au ** Email: m.stevens@imperial.ac.uk

**Materials and Methods**

The lipids POPC, POG and POPA were purchased from Avanti Polar Lipids, Alabaster, USA in lyophilized powder form (purity >99%), and used without further purification. Lipids were stored at -20 °C and warmed to room temperature before use. Phosphate buffered saline (140 mM NaCl, 10 mM $Na_3PO_4$, 2.68 mM KCl, pH 7.45) was prepared from commercially available tablets (Life Technologies, Carlsbad, California, USA) and filtered through a 0.2 μm membrane before use. All other chemicals and phospholipases were purchased from Sigma Aldrich and used as supplied.

***Liposome formulation:*** Liposomes were prepared by the freeze-thaw method and extruded to the desired size. Thin films were prepared by evaporating chloroform solutions of POPC. After drying *in vacuo* overnight, films were incubated for 30 min with 1 mL phosphate-buffered saline solution (PBS) at pH 7.4 (lipid concentration approx. 2.7 mM (SPR experiments) or 27 mM (SANS experiments)). Subsequently five freeze-thaw cycles were carried out using liquid nitrogen and a 40 ˚C water bath. The resulting multilamellar vesicles were extruded 15 times using a micro-extruder (Avanti Polar Lipids) and polycarbonate membranes (Whatman Nucleopore) with 200 nm pores. When required they were also further extruded 15 times through 50 nm membranes. For SPR experiments, liposome formulations were diluted to 0.5 mM total lipid concentration in PBS.

***SANS measurements:*** Measurements were carried out at both the SANS2D and Larmor beamlines of the ISIS pulsed neutron source at the Rutherford Appleton Laboratory, Didcot, UK, using a sample changer and 2 mm path length quartz cuvette cells, sample volume 350 μL. Time resolved scattering measurements for 50 nm POPC liposomes (4 mM final lipid concentration) with either phospholipase C from *Bacillus cereus* or phospholipase D from *Streptomyces chromofuscus*, (final activity 12.5 U/mL) were collected on SANS2D. Time-resolved scattering measurements were collected on Larmor for 50 nm POPC liposomes (4 mM final lipid concentration) with phospholipase D from *Arachis hypegaea*, (final activity 12.5 U/mL). The solvent was PBS with 0.5 mM $CaCl_2$, prepared in 90% $D_2O$, 10% $H_2O$ to reduce incoherent scattering from $H_2O$ and give good scattering contrast. Typical data collection times on SANS2D were 15 min. The beamline was configured with $L_1 = L_2 = 4$ m pinhole collimation and sample-detector distances to give a scattering vector $Q = (4\pi/\lambda)\sin(\theta/2)$ range of 0.004 to 0.8 $Å^{-1}$, where θ is the scattering angle and neutrons of wavelengths λ of 1.75 to 16.5 Å were used simultaneously by time of flight. Measurements on Larmor were carried out in event mode and the wavelength and Q range for this experiment were 0.9 – 12.5 Å and 0.004 – 0.8 $Å^{-1}$ respectively. The instrument was in the 4 m sample-detector configuration, with A1=20$mm^2$, S1=14$mm^2$, and a sample aperture of 6mm (horizontal) by 8mm (vertical). Data reduction was performed using Mantid[1] and scattering simulations fitted using SasView v3.0.[2] All measurements were fitted using a custom model, taking the sum of two MultiShellVesicle models and fixing the parameters to have one (unilamellar component, see Table 1) and two (bilamellar component) shells respectively (see below for further details).

***SAXS measurements:*** Mixtures of POPC:POG and POPC:POPA at 100:0, 90:10, 50:50 and 10:90 mol% were co-dissolved in chloroform which was evaporated under a stream of nitrogen, then lyophilized overnight for a minimum of 12 h to remove any residual solvent. Mixtures were hydrated

in: a) POPC:POG mixtures, PBS w/w to 60 wt% and b) POPC:POPA mixtures, PBS or pure water (Gibco) w/w to 80 wt%. Samples were sealed and heat cycled 20 times between -196°C and 60 °C. SAXS data was obtained at 25 °C at Diamond Light Source, UK, using beamline I22, with samples mounted in glass capillaries (Capillary Tube Supplies Ltd SGCT 1.5 mm). The beamline was configured at an X-ray energy of 18 keV and 3.7 m sample to detector distance to give a scattering vector $S = (2/\lambda)\sin(\theta/2) = Q/(2\pi)$ range of 6.5 x $10^{-5}$ to 1 x $10^{-1}$ $Å^{-1}$, where θ is the scattering angle and the X-ray wavelength λ is 0.6902 Å. Images were analyzed using the AXcess software package.[3] Briefly, the two-dimensional SAXS images were radially integrated to give one-dimensional diffraction patterns. The Bragg peaks were then fitted using Gaussian functions and indexed by comparison to characteristic peak spacings from known lipid structures.

***All-Atom Simulations:*** The lipid bilayer was initially created with equilibrated POPC lipids using CHARMM-GUI.[4] A membrane bilayer with 70 POPC lipids in each leaflet was solvated with water molecules, after which 150 mM NaCl was added and the system was equilibrated for 100 ns. The equilibrated POPC lipid bilayer was converted to 10% and 50% POG or POPA systems with unit cell sizes around 65.5 × 65.5 × 89.5 $Å^3$ comprising ~40000 atoms. All defect systems were run for 200 ns to equilibrate and the last 100 ns were used for analysis.

MD simulations were performed using the NAMD code (version 2.9)[5] with the CHARMM36 lipid,[6] and TIP3P water and NBFIX ion parameters as defined by the CHARMM36 FF. The POG head group (OH) parameters were taken from CHARMM General FF and charges in the OH group were optimized. For POPA, the topology and parameters for the PA head group were taken from the CHARMM36 lipid.[6] Simulations were performed in the NPT ensemble with the temperature and pressure maintained at 300 K and 1 atm, respectively, via Langevin coupling with damping coefficient of 5 $ps^{-1}$. All bonds to hydrogen atoms were maintained using the SHAKE algorithm.[7] Periodic boundary conditions were employed with the particle-mesh Ewald algorithm[8] to compute the long-range electrostatic interactions. Lennard-Jones (LJ) potential was switched off within 10-12 Å using a force-switching function. A non-bonded pair list cutoff of 16 Å was used. A time step of 2 fs was maintained throughout the simulations.

***Surface Plasmon Resonance*:** SPR measurements were carried out using a Biacore 3000 and an L1 chip (Sensor Chip L1, GE Healthcare), at 25 ˚C. All solutions were degassed overnight prior to use. Flow cells 1 and 2 (Fc1 and Fc2) of a new L1 chip were cleaned with PBS (350 s, flow rate 100 µL/min) followed by 20 mM CHAPS solution in deionized water (3 x 50 uL injections, flow rate 100 µL/min). The chip was further stabilized with PBS (flow rate 100 µL/min) for 1 h before use. Using a flow rate of 10 µL/min, 200 or 50 nm POPC liposomes were immobilized onto Fc2 in a 50 µL injection, followed by two 10 µL injections of 50 mM NaOH in deionized water to remove loosely bound liposomes. After washing with PBS (300 µL, 100 µL/min), PLC from *Clostridium perfringens (C. welchii)*, PLC from *Bacillus cereus* or PLD from *Arachis hypegaea* (50 mU/mL in PBS with 0.5 mM $CaCl_2$) was injected in 2 or 3 x 325 µL injections (flow rate 40 µL/min). Finally, the chip was regenerated by washing with PBS (400 µL) followed by 3 x 40 µL injections of 20 mM CHAPS in deionized water (all at flow rate 40 µL/min). As a control, Fc1 was treated in the same manner, with

the exception of liposome injection where PBS only was injected. Each enzyme experiment was repeated in triplicate.

***Raman spectroscopy of liposomes incubated with PLC and PLD:*** 200 nm POPC liposomes (2.5 mg/mL lipid concentration) were incubated for 1 h at 37 ˚C with PLC from *Clostridium perfringens (C. welchii)*, or PLD from *Arachis hypegaea* (both 50 mU/mL), in PBS buffer containing 0.5 mM $CaCl_2$. Subsequently 5 µL of each suspension was pipetted onto a 1 $cm^2$ $MgF_2$ slide and evaporated to dryness. A control sample of POPC liposomes incubated without enzyme was also prepared. Raman spectroscopy was carried out on a Witec Alpha 300+ (532 nm laser, 1800 g/mm grating) with laser power set to 1.5 mW and 5 sec integration time. Three to four spectra from different sample positions were collected, the background was corrected using a polynomial subtraction and the background corrected spectra were averaged.

**Safety Statement**

No unexpected or unusually high safety hazards were encountered**.**

SANS data were fitted using a multilayer vesicle model in the SasView v3.0.[2] program.

The absolute scattering intensity I(Q) was calculated as the sum of terms for volume fractions $\varphi_1$ and $\varphi_2$ of uni-lamellar and bi-lamellar vesicles, together with a flat background to allow for residual incoherent and/or inelastic scatter. The code fits the total volume fractions of polydisperse particles, but these can be converted to number densities (particles per unit volume) or volume fractions of material in the shells.

$I(Q) = \varphi_1 P_1(Q) + \varphi_2 P_2(Q) + BKG$

$$P_i(Q) = \frac{1}{V_i}\int F_i(Q, r_{ci})^2 . N(r_{ci}) \mathrm{d}r_{ci}$$

Where $V_i$ is an appropriate normalization factor for polydispersity function N(r). For spherical shells of thickness T, with gaps G, (thus a "d-spacing" of T+G):

$$F_i(Q, r_c) = (\rho_c - \rho_s) \sum_{j=1}^{i} ( f(Q, r_c + (j-1)(T+G)) - f(Q, r_c + (j-1)(T+G) + T))$$

$$f(Q, r) = \frac{4\pi r^3}{3} \frac{(\sin(Qr) - Qr.cos(Qr)}{(Qr)^3}$$

Where the shells have neutron scattering length density of $\rho_s$ and the bulk solvent core $\rho_c$ The uni- and bi-lamellar vesicles were allowed to have different core radii, but their Gaussian polydispersity functions were kept at standard deviations of 12%.

For a simple spherical particle system, discounting any polydispersity, the volume fraction $\varphi_i$ of a particle population becomes:

$$\varphi_i = N_i . V_i$$

where $N_i$ is the number of particles and $V_i$ is the volume per particle/shell. Given particle core radius ($r_c$), and bilayer thickness (T), one can calculate $V_{p,i}$ and $V_{s,i}$, respectively the total volume per particle and shell volume per particle. Thus, the proportion of bilamellar sub-population can be calculated as a function of total particle volume (see Table 1), particle number and lipid volume (see Table S1).

Table S1. Fitted SANS parameters and simple estimates of the particle number and lipid volume ratios of the bilamellar vesicle component. Lengths and volumes are in Å and $Å^3$ respectively.

Unilamellar component

| Time (min) | $\varphi_1$ | $r_{core\ 1}$ | $T_1$ | $V_{p1}$ | $V_{s1}$ | $N_1$ | $\varphi_{s1}$ |
|---|---|---|---|---|---|---|---|
| 0 | 1.07E-02 | 583 | 36 | 9.91E+08 | 1.61E+08 | 1.08E-11 | 1.74E-03 |
| 15 | 8.16E-03 | 586 | 35 | 1.00E+09 | 1.60E+08 | 8.13E-12 | 1.30E-03 |
| 120 | 7.09E-03 | 1118 | 30 | 6.33E+09 | 4.77E+08 | 1.12E-12 | 5.35E-04 |
| 230 | 4.39E-03 | 980 | 31 | 4.33E+09 | 3.86E+08 | 1.01E-12 | 3.91E-04 |
| 460 | 4.05E-03 | 800 | 18 | 2.29E+09 | 1.48E+08 | 1.77E-12 | 2.62E-04 |
| 700 | 2.05E-03 | 700 | 19 | 1.56E+09 | 1.18E+08 | 1.32E-12 | 1.56E-04 |

Bilamellar component

| Time (min) | $\varphi_2$ | $r_{core\ 2}$ | $T_2$ | G | $V_{p2}$ | $V_{s2}$ | $N_2$ | $\varphi_{s2}$ |
|---|---|---|---|---|---|---|---|---|
| 0 | 8.06E-04 | 230 | 36 | 25 | 1.47E+08 | 7.11E+07 | 5.50E-12 | 3.91E-04 |
| 15 | 8.42E-04 | 230 | 36 | 25 | 1.47E+08 | 7.11E+07 | 5.74E-12 | 4.08E-04 |
| 120 | 5.76E-04 | 281 | 38 | 25 | 2.33E+08 | 1.06E+08 | 2.47E-12 | 2.61E-04 |
| 230 | 3.63E-04 | 310 | 37 | 25 | 2.87E+08 | 1.21E+08 | 1.27E-12 | 1.54E-04 |
| 460 | 3.65E-04 | 310 | 37 | 25 | 2.87E+08 | 1.21E+08 | 1.27E-12 | 1.54E-04 |
| 700 | 2.23E-04 | 323 | 45 | 25 | 3.51E+08 | 1.65E+08 | 6.35E-13 | 1.05E-04 |

| | NUMBER | SHELL VOLUME |
|---|---|---|
| Time (min) | $N_2/(N_1+N_2)$ | $\varphi_{s2}/(\varphi_{s1}+\varphi_{s2})$ |
| 0 | 0.338 | 0.183 |
| 15 | 0.414 | 0.238 |
| 120 | 0.688 | 0.328 |
| 230 | 0.555 | 0.282 |
| 460 | 0.418 | 0.371 |
| 700 | 0.325 | 0.402 |

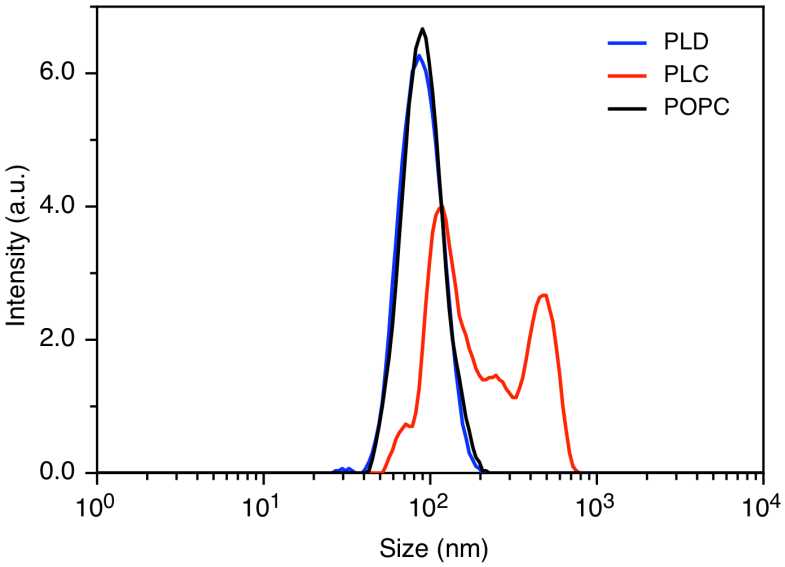


Figure S1. Dynamic Light Scattering of SANS samples after acquisition of SANS data (Figure 2). Shown are intensity-based measurements of POPC vesicles (black), POPC vesicles incubated with PLC from *Bacillus cereus* (red) and POPC vesicles incubated with PLD (blue), diluted to 1% of the measured SANS concentration in PBS. Data was acquired using a Malvern Zetasizer Nano S.

Since many conventional phospholipase assays measure enzyme activity on free lipids in solution, and were therefore not appropriate in this study, we used SPR to determine enzyme-induced cleavage of the phosphorous-oxygen bonds of POPC vesicles (Figure S2) as a qualitative means of comparing enzyme activity. Specifically, we used a Biacore L1 chip, which is a commercially available dextran-coated gold chip modified with alkyl chains, designed for label-free attachment of liposomes. While it is possible for vesicles to fuse and form a homogeneous membrane bilayer on the chip surface, in general the formation of monolayers of intact liposomes is observed on L1 chips.[9] Here, our choice of liposome formulations and loading conditions, coupled with the observed changes in response units (RU) during the deposition step, indicate adhesion of intact vesicles in contrast to the formation of a membrane bilayer.

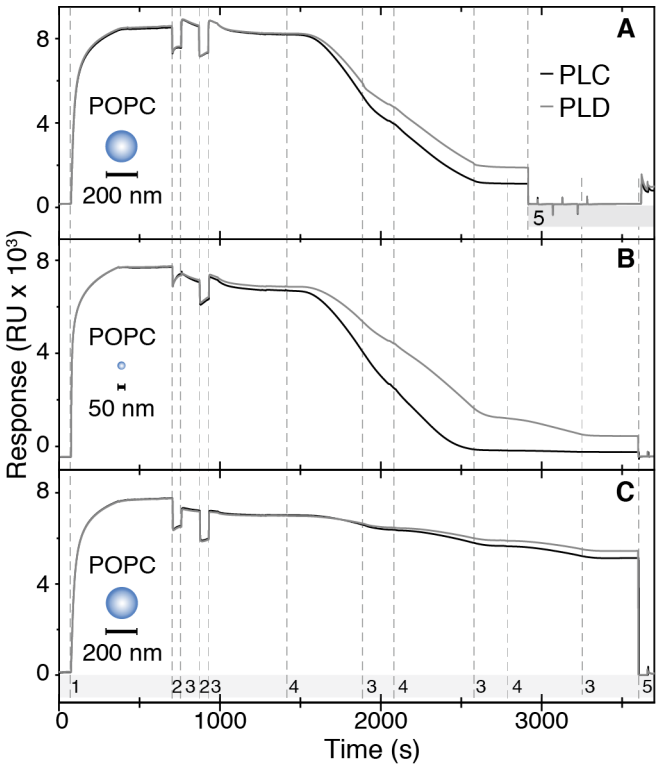


Figure S2. SPR of POPC liposomes in presence of PLC or PLD. A: 200 nm POPC liposomes incubated with 10 mU/mL PLC or PLD. B: 50 nm POPC liposomes incubated with 10 mU/mL PLC or PLD. C: 200 nm POPC liposomes incubated with 100 µU/mL PLC or PLD. Injection 1, liposomes (300 s followed by PBS); 2, NaOH (50 mM); 3, PBS; 4, PLC or PLD; 5, CHAPS.

After binding liposomes to the chip, buffer containing 10 mU/mL of either PLC or PLD was passed over the chip surface. On addition of enzyme, we did not observe an increase in RU corresponding to enzyme-substrate binding ($K_{on}$). The PLC and PLD activities used in these SPR experiments correspond to 5-50 pgP/mm$^3$, which is close to the limit of detection of enzyme binding to the SPR chip. Given this and the increased distance from the gold surface of the chip compared to standard protein binding affinity measurements (caused by the presence of liposomes), it is not surprising that the enzyme-liposome binding events are not observed here.

In all experiments at 10 mU/mL PL activity, a lag time of around 2 min was observed after enzyme addition before a decrease in RU. Similar lag times are reported in the literature for several phospholipases.[10-12] During this time it is likely that structural rearrangement is ongoing with increasing concentration of DAG/PA, until a critical rearrangement at which time there is either a burst in enzyme activity or a large-scale change in lipid packing, and the vesicles detach from the chip. We observed the latter in SAXS data (see Figure S7) for the PC:DAG system, with the evolution of a liposome-destabilizing hexagonal phase followed by a pure Fd3m micellar phase above a critical concentration of DAG. Likewise, at very high conversions of PC (POPC transition melting temperature, $T_m$ = 2 ˚C) to PA (POPA $T_m$ = 28 ˚C), one would expect a phase change from the liquid disordered to gel phase. In both PLC and PLD, flip-flop induced relaxation of bending energy arising from an asymmetric membrane[13] may also play a role in liposome detachment. Finally, the flow rate during enzyme addition is 40 µL/min, and therefore re-binding of detached vesicles to the chip is highly unlikely.

In all cases, the rate of cleavage (determined by the rate of decrease in RU) was greater for PLC than PLD. This could be perhaps justified by the fact that the mass of the DAG cleavage product from PC reaction with PLC is smaller than that of the PA reaction product from PC reaction with PLD. However, it is more likely due to differences in activity of the enzymes in these specific conditions. This is corroborated by our observations that, although it followed the same trend, the same experiment with PLC from *Bacillus cereus* led to a slower rate of detachment than either of the two sensorgrams shown in Figure S2 (raw data available). Reducing enzyme activity (Figure S2C) leads to a less pronounced overall change in RU, but not an appreciable decrease in the lag phase time before decrease in RU. Due to the almost stoichiometric ratio of enzyme molecules to liposomes, it is possible that there are two vesicle sub-populations representing one population with bound enzyme and one without. Similar systems have previously been studied by total internal reflection fluorescence microscopy and deconvoluted to characterize single enzyme activity on single liposomes.[14] This explains the unchanged lag phase between different enzyme concentrations, because it represents the time before detachment of vesicles having been acted on by a single enzyme.

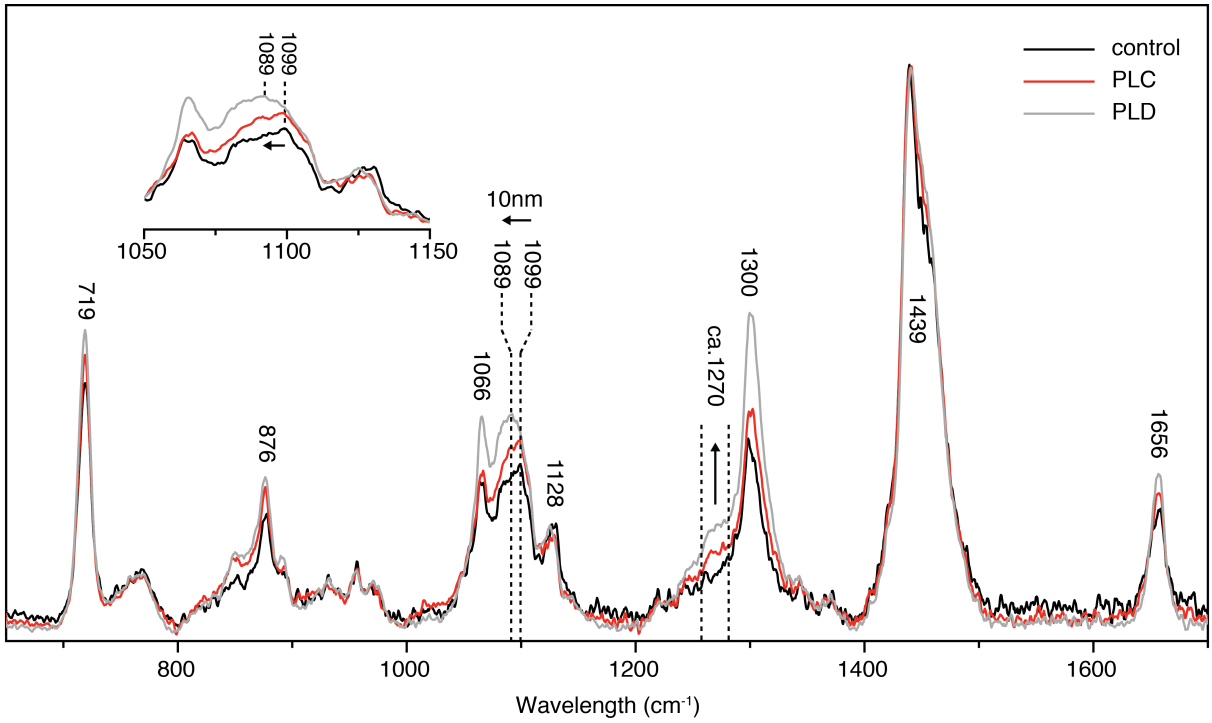


Figure S3. Averaged Raman spectra of POPC liposomes incubated with PLC or PLD for 1 h. The peak at 1099 $cm^{-1}$ attributed to the $PO_2$ group[15] shows pronounced changes in both enzyme-treated samples (see inset). Specifically, it shifts 10 $cm^{-1}$ to the left in the case of PLD, indicative of changes to its local chemical environment. A shoulder at around 1270 $cm^{-1}$ attributed to unsaturated fatty acids[15] develops in both the PLC and PLD treated samples.

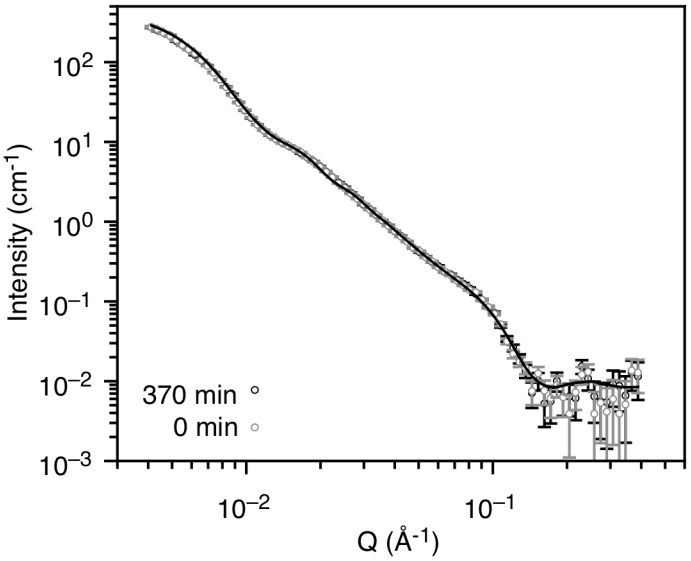


Figure S4. Neutron scattering data of 50 nm POPC vesicles in the presence of PLD from *Arachis hypegaea* before enzyme addition (0 min) and at 370 min incubation. As in the case of PLD from *Streptomyces chromofuscus* (see Figure 2), no change in membrane bilayer thickness or vesicle morphology was observed even after 370 min incubation. Here, the fitted SANS parameters for both the 0 and 370 min time points are the same and correspond to the 0 min fitted parameters presented in Table 1.

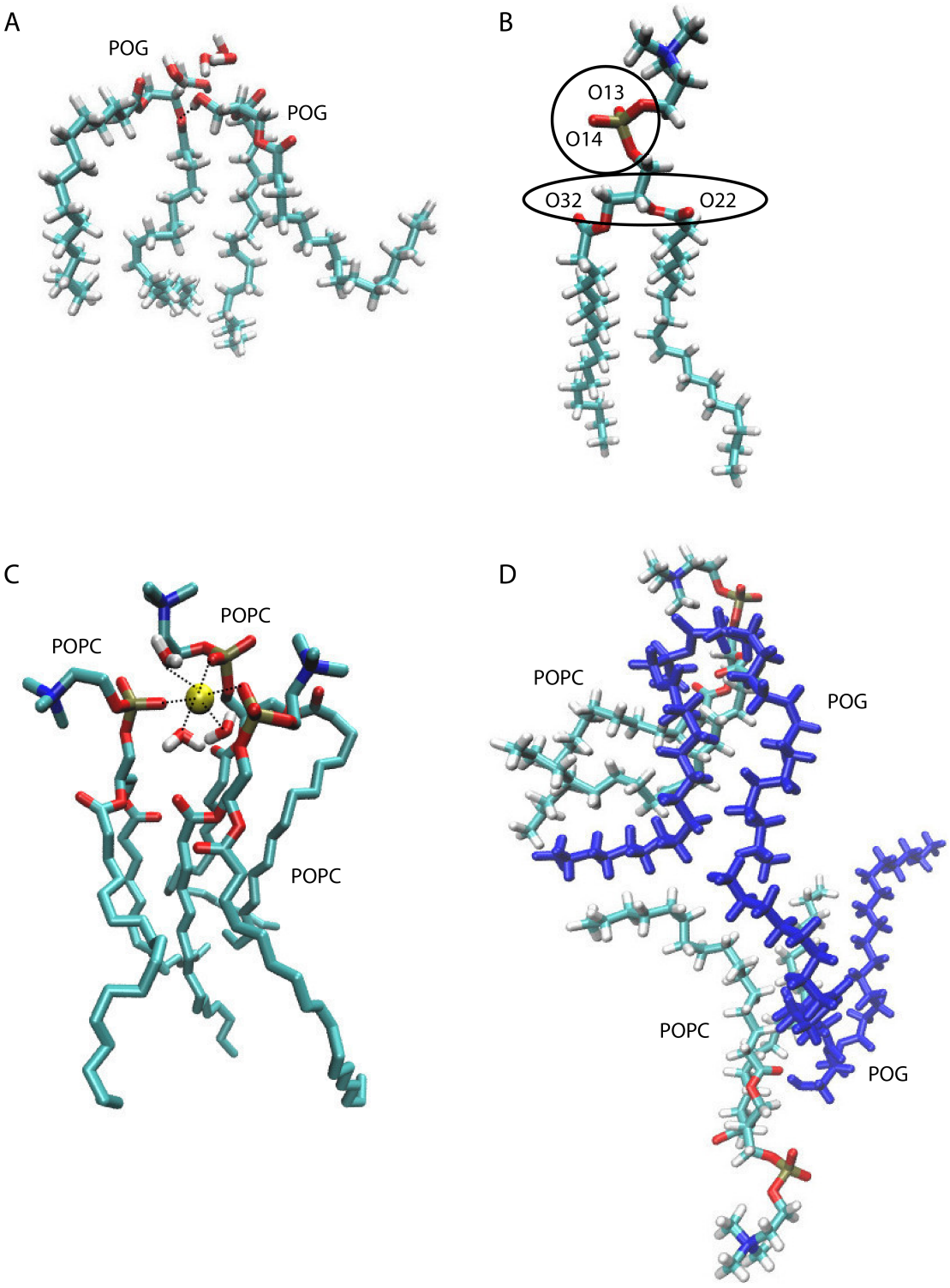


Figure S5. MD snapshots of typical lipid complexes within the bilayer. (A) Snapshot of hydrogen bond between two POG molecules in a POPC:POG (1:1) bilayer. (B) The positions of phosphate oxygens (O13, O14) and carbonyl oxygens (O22, O32) in POPC. (C) Snapshot of $Na^+$ ion (yellow) coordination with three POPC residues and three water molecules. (D) Snapshot of tail mismatch in POPC:POG (9:1) system where the POG residues are represented in blue for clarity.

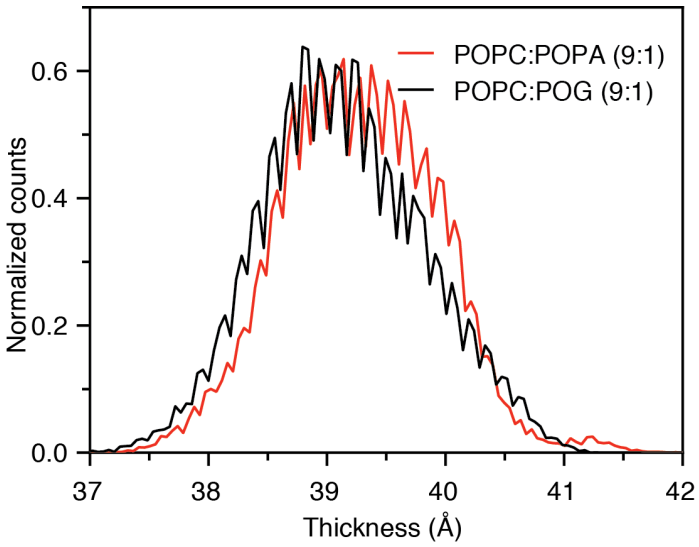


Figure S6. Normalized distribution of bilayer thickness for 100-200 ns simulation (considering phosphate groups in both leaflets). Red trace is the thickness distribution of a POPC:POPA (9:1) bilayer and black is for the POPC:POG (9:1) bilayer. The distributions are centered at ~39.2 Å.

Movie S1. POG head group -OH forms a hydrogen bond with the carbonyl oxygen of POPC in POPC:POG (9:1) bilayers. Only heavy atoms of a POG and a POPC molecule are shown.

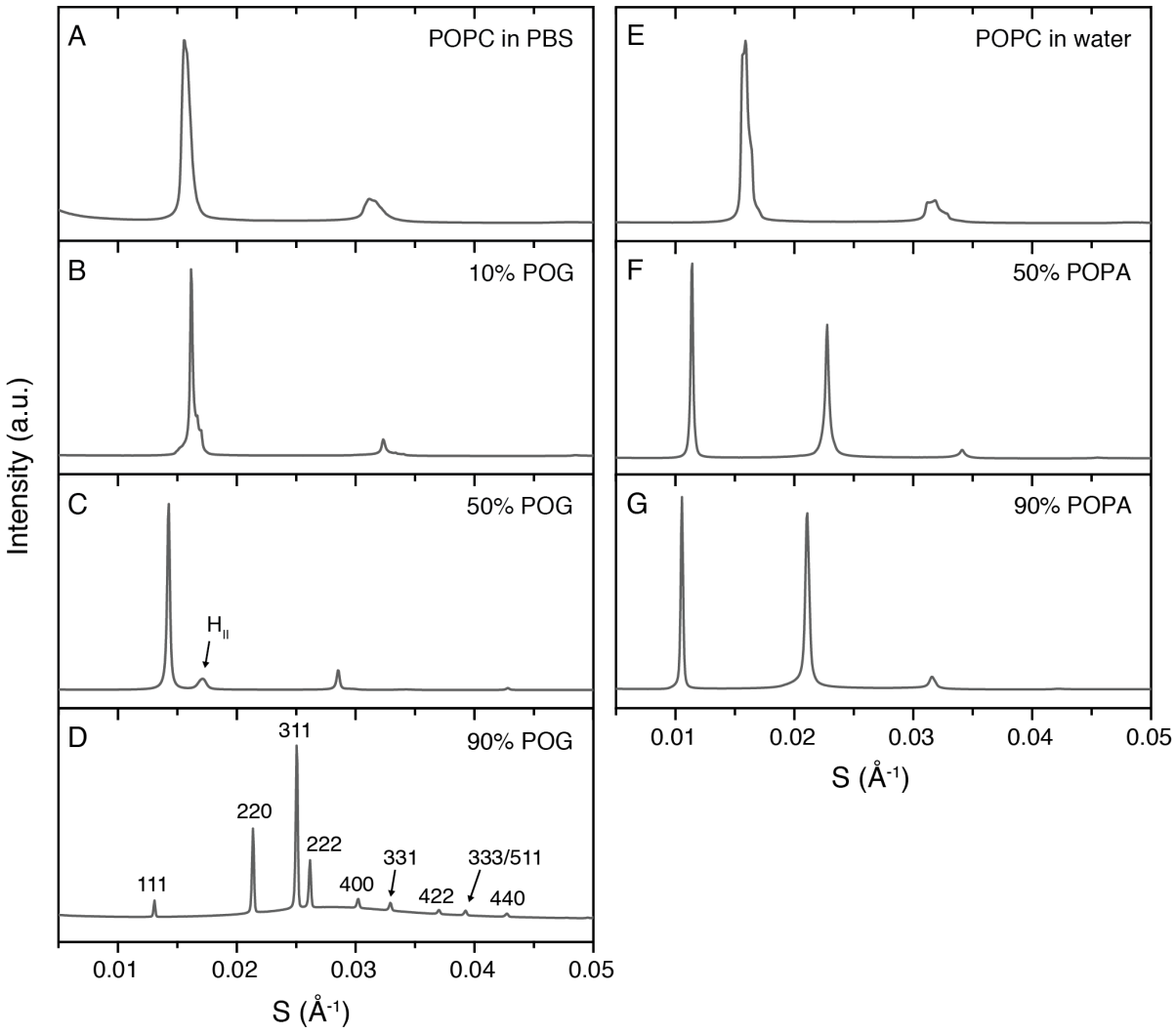


Figure S7. SAXS studies of bulk lipid mixtures. (A) POPC hydrated in PBS; (B) POPC with 10 mol% POG hydrated in PBS; (C) POPC with 50 mol% POG hydrated in PBS; (D) POPC with 90 mol% POG hydrated in PBS (annotations show peak Miller indexes for Fd3m phase); (E) POPC hydrated in water; (F) POPC with 50 mol% POPA hydrated in water; and (G) POPC with 90 mol% POPA hydrated in water. The slight splitting in (A), (B) and (E) is due to either incomplete mixing or slight degradation of the POPC lipid. The calculated D-spacings of 63.81 ± 0.03 Å (A) and 63.05 ± 0.30 Å (E) are in agreement with the literature.[16]

## REFERENCES


1. Arnold, O.; Bilheux, J. C.; Borreguero, J. M.; Buts, A.; Campbell, S. I.; Chapon, L.; Doucet, M.; Draper, N.; Ferraz Leal, R.; Gigg, M. A.*, et al.*, Mantid—Data Analysis and Visualization Package for Neutron Scattering and M Sr Experiments. *Nucl. Instrum. Methods Phys. Res. A* **2014,** *764*, 156-166.
2. http://www.sasview.org/. (accessed 27th July 2015).
3. Seddon, J. M.; Squires, A. M.; Conn, C. E.; Ces, O.; Heron, A. J.; Mulet, X.; Shearman, G. C.; Templer, R. H., Pressure-Jump X-Ray Studies of Liquid Crystal Transitions in Lipids. *Philos. Trans. Royal Soc. A* **2006,** *364*, 2635-2655.
4. Jo, S.; Kim, T.; Iyer, V. G.; Im, W., Charmm-Gui: A Web-Based Graphical User Interface for Charmm. *J. Comput. Chem.* **2008,** *29*, 1859-1865.
5. Phillips, J. C.; Braun, R.; Wang, W.; Gumbart, J.; Tajkhorshid, E.; Villa, E.; Chipot, C.; Skeel, R. D.; Kale, L.; Schulten, K., Scalable Molecular Dynamics with Namd. *Journal of Computational Chemistry* **2005,** *26*, 1781-1802.
6. Klauda, J. B.; Venable, R. M.; Freites, J. A.; O' Connor, J. W.; Tobias, D. J.; Mondragon-Ramirez, C.; Vorobyov, I.; MacKerell, A. D. J.; Pastor, R. W., Update of the Charmm All-Atom Additive Force Field for Lipids: Validation on Six. *J. Phys. Chem. B* **2010,** *114*, 7830-7843.
7. Ryckaert, J.-P.; Ciccotti, G.; Berendsen, H. J., Numerical Integration of the Cartesian Equations of Motion of a System with Constraints: Molecular Dynamics of N-Alkanes. *J. Comput. Phys.* **1977,** *23*, 327-341.
8. Darden, T.; York, D.; Pedersen, L., Particle Mesh Ewald: An N·Log(N) Method for Ewald Sums in Large Systems. *J. Chem. Phys.* **1993,** *98*, 10089-10092.
9. Anderluh, G.; Besenicar, M.; Kladnik, A.; Lakey, J. H.; Macek, P., Properties of Nonfused Liposomes Immobilized on an L1 Biacore Chip and Their Permeabilization by a Eukaryotic Pore-Forming Toxin. *Anal. Biochem.* **2005,** *344*, 43-52.
10. Urbina, P.; Flores-Diaz, M.; Alape-Giron, A.; Alonso, A.; Goni, F. M., Effects of Bilayer Composition and Physical Properties on the Phospholipase C and Sphingomyelinase Activities of Clostridium Perfringens Alpha-Toxin. *Biochimica et Biophysica Acta-Biomembranes* **2011,** *1808*, 279-286.
11. Aili, D.; Mager, M.; Roche, D.; Stevens, M. M., Hybrid Nanoparticle-Liposome Detection of Phospholipase Activity. *Nano Lett.* **2011,** *11*, 1401-1405.
12. Wagner, K.; Brezesinski, G., Phospholipases to Recognize Model Membrane Structures on a Molecular Length Scale. *Curr. Opin. Colloid Interface Sci* **2008,** *13*, 47-53.
13. Bruckner, R. J.; Mansy, S. S.; Ricardo, A.; Mahadevan, L.; Szostak, J. W., Flip-Flop-Induced Relaxation of Bending Energy: Implications for Membrane Remodeling. *Biophys. J.* **2009,** *97*, 3113-3122.
14. Tabaei, S. R.; Rabe, M.; Zetterberg, H.; Zhdanov, V. P.; Hook, F., Single Lipid Vesicle Assay for Characterizing Single-Enzyme Kinetics of Phospholipid Hydrolysis in a Complex Biological Fluid. *J. Am. Chem. Soc.* **2013,** *135*, 14151-14158.
15. Movasaghi, Z.; Rehman, S.; Rehman, I. U., Raman Spectroscopy of Biological Tissues. *Appl. Spectrosc. Rev.* **2007,** *42*, 493-541.
16. Johnson, M.; Seifert, S.; Petrache, H. I.; Kimble-Hill, A. C., Phase Coexistence in Single-Lipid Membranes Induced by Buffering Agents. *Langmuir* **2014,** *30*, 9880-9885.